Scanning Probe Lithography. 3. Nanometer-Scale Electrochemical Patterning of Au and Organic Resists in the Absence of Intentionally Added Solvents or Electrolytes

Jonathan K. Schoer, Francis P. Zamborini, and Richard M. Crooks*

Department of Chemistry, Texas A & M University, College Station, Texas 77845-3255

Received: January 29, 1996; In Final Form: April 20, 1996[⊗]

Here we provide evidence that the principal mechanism responsible for scanning tunneling microscope (STM)-induced removal (or deposition) of material from organic thin films in air is electrochemical in nature. In experiments conducted in high-humidity (>∼70% relative humidity) ambients, patterning proceeds at biases above ∼+2.3 V because a thin layer of water adsorbed to the tip and surface establishes an ultra-thin-layer electrochemical cell. The low-energy self-assembled monolayer (SAM) restricts the dimensions of the highly resistive solution in the tip−sample gap and confines the patterning to the immediate vicinity of the tip, passivates unetched regions of the Au(111) substrate, and retards the surface mobility of Au atoms thereby stabilizing the patterns. In the absence of SAMs, patterns in nominally naked Au(111) are irreproducible and rapidly anneal to their pre-etch form. In low-humidity (<∼25% relative humidity) ambients there is insufficient water on the SAM surface to support Faradaic electrochemistry and insignificant patterning is observed at sample biases up to +5.0 V. We observed a bias threshold for patterning that is dependent on the composition of the tip−sample gap, but found that the bias threshold is essentially independent of the tunneling current. Using this scanning tunneling microscope-induced electrochemical patterning, we are able to reproducibly and selectively deposit or remove material from the surface to yield features having critical dimensions of less than 10 nm.

Introduction

Here we provide evidence that the principal mechanism responsible for scanning tunneling microscope (STM)-induced removal (or deposition) of material from organic thin films in air is electrochemical in nature. Our results are important for two primary reasons. First, the data indicate that Faradaic electron transfer can dominate processes occurring in the intragap region of an STM operating in air. Second, our observations provide a convenient method for studying electrochemical phenomena on a 1−100 nm length scale and electrochemically altering volumes smaller than 100 nm[3].

We[1] and others[2−4] have previously speculated that an electrochemical mechanism could be responsible for STM-induced surface transformations in air. In air, a thin layer of water is present on most surfaces, and, together with adventitious or electrogenerated impurities, this layer can act as an electrolyte solution to support low-current electrochemical processes. For example, in studies of STM-induced modification of nominally naked conducting surfaces such as graphite[2,5−8] and titanium,[9−11] it was proposed that water was reduced at the STM tip (cathode) and that patterning resulted from oxidation of the substrate (anode).

We have previously reported on STM-induced lithography of *n*-alkanethiol self-assembled monolayers (SAMs) confined to Au surfaces and applications of the resulting patterns.[1,12−14] To better control patterning and to further elucidate the nature of the processes responsible for the tip-induced surface modification, we examined the impact of various experimental parameters, including the chemical nature of the tip−substrate gap.[15,16] Here we focus on scanning-probe-induced electrochemical patterning of nominally naked Au(111) and *n*-alkanethiol-coated Au(111) surfaces in controlled-humidity ambients. In many respects our results are similar to those obtained using the scanning electrochemical microscope (SECM).[17−22] However, the nature of the interfacial chemistry in our experiments is less well defined. This complication is compensated by much higher spatial resolution.

Experimental Section

Chemicals. Octadecyl mercaptan (ODM), $HS(CH_2)_{17}CH_3$ (Aldrich, 98%), nonyl mercaptan (NM), $HS(CH_2)_8CH_3$ (Aldrich, 98%), and 100% ethanol were used as received.

Sample Preparation. We prepared SAM-modified substrates as described previously.[13,14,23−27] Briefly, melting a Au wire (0.25 mm diameter, 99.9985% purity, Johnson Matthey) in a H_2/O_2 flame forms a 1−1.5 mm diameter ball at the end of the wire. The ball has a few elliptical Au(111) facets (long axis ∼300 μm) on its surface which contain atomically flat terraces up to 1 μm in width. After electrochemically cleaning, polishing, and annealing a ball, we immersed it in ethanolic solutions of the desired organomercaptan (∼2.0 mM) for 16−20 h. We then removed the SAM-coated Au ball, rinsed it with ethanol, and dried it under a gentle stream of nitrogen.

STM Data Acquisition. We used a NanoScope III STM (Digital Instruments, Santa Barbara, CA) for all experiments. Tips were mechanically cut from Pt/Ir (80/20%) wire, and substrates were mounted into a custom-fabricated holder.[28] We obtained all images using a D scanner (∼12 μm scan range) and instrumental conditions that minimize tip-induced surface damage: +0.3 V sample bias, 150 pA tunneling current, 4 Hz scan rate, and 256 × 256 pixel resolution.[15] We refer to these as standard imaging conditions (SIC) in the text. The entire microscope assembly was housed inside a custom-designed, polycarbonate, environmental chamber that was constantly purged with nitrogen (99.995%) or air. The humidity and temperature were monitored with a combination humidity and temperature indicator (Vaisala, Model HMI 31).

* Author to whom correspondence should be addressed. E-Mail: Crooks@chemvx.tamu.edu. Telephone: 409-845-5629. FAX: 409-845-1399.

[⊗] Abstract published in *Advance ACS Abstracts,* June 1, 1996.

S0022-3654(96)00271-7 CCC: $12.00

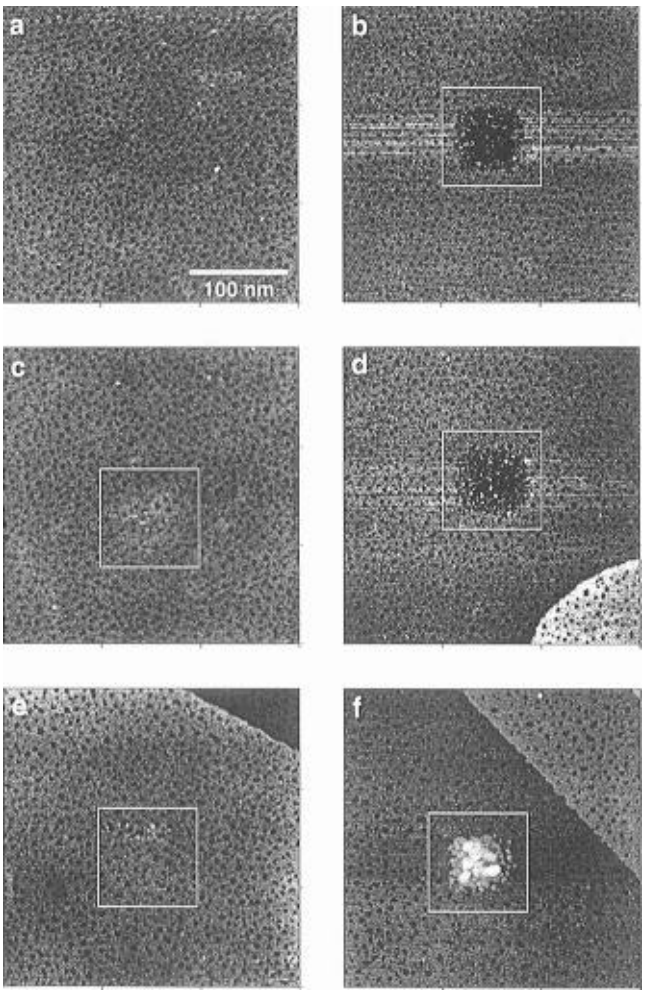

Figure 1. 300 nm × 300 nm STM images of *n*-octadecyl mercaptan (ODM) SAMs before and after patterning a nominally 50 nm × 50 nm feature. Table 1 lists the patterning conditions used for each part of the figure and some physical data describing the resulting patterns. The gray scale is 2 nm. The white boxes in frames b−f are 100 nm × 100 nm and are centered on the patterns. Patterning proceeds only in humid environments regardless of the polarity of the applied bias.

STM-Induced Patterning. We prepared 50 nm × 50 nm patterns by scanning the ODM-coated Au surface four times at high scan rate (41 Hz) and bias (±3.0 V) with the *z*-piezo feedback of the STM enabled. Smaller patterns (<10 nm) were prepared by applying a 1 s bias pulse (tip stationary) with the *z*-piezo feedback of the STM disabled. During patterning the tunneling current and resolution were set to 150 pA and 256 × 256 pixels, respectively. A positive bias indicates electron tunneling from the tip to the substrate.

Results and Discussion

Figure 1 consists of a series of 300 nm × 300 nm STM images of ODM-coated Au(111) surfaces before and after patterning areas nominally 50 nm × 50 nm in size. Table 1 lists the conditions used to fabricate the features in each part of Figure 1 and also some physical characteristics of the resulting patterns. The data in Figure 1 and Table 1 are typical of many such features we have prepared, but under nominally identical conditions the root-mean square (RMS) roughness factor (RRF)[29] generally ranges between 1.8 and 2.8, the depth ranges between 0.22 nm and 0.45 nm, and the lateral dimensions vary by <∼10% between experiments. Figure 1a is an image of an unpatterned *n*-alkanethiol-coated Au(111) surface.[30] It is characterized by an atomically smooth terrace covered by numerous 2−10-nm-diameter indigenous pits that are approximately 0.24 nm deep, which we and others have previously shown result from adsorbate-driven Au−surface reorganization.[31−38] Figure 1b shows the same surface region after patterning a nominally 50 nm × 50 nm feature at +3.0 V (substrate positive) in air having a relative humidity (RH) of 75%. The surface is generally unchanged from Figure 1a except for the presence of the patterned feature enclosed in the box. The white streaks on either side of the pattern are imaging artifacts, not real surface features. The RRF[29] (2.4) and depth[39] (−0.29 nm) of the feature are typical of our results immediately following patterning (Table 1). The roughness of the feature compared to the unpatterned surface is consistent with electrochemical roughening of the surface and generation of loosely bound debris within the pattern.[12,40−47]

TABLE 1: Conditions Used To Pattern the Features Shown in Figure 1 and Some Physical Characteristics of the Patterns

part	patterning environment	relative humidity[a] (%)	patterning bias (V)	RMS roughness factor[29]	net pattern depth[39] (nm)
a	air	75	prepattern	0.95	0.00
b	air	75	+3.0	2.37	−0.29
c	air	6.6	+3.0	1.00	+0.06
d	N_2	78	+3.0	2.22	−0.25
e	N_2	5.0	+3.0	1.00	+0.01
f	air	78	−3.0	2.34	+0.24

[a] The temperature for these experiments varied between 25 and 26.7 °C, but was typically 25.5 °C.

The feature depth is only about 10% of the thickness of the monolayer (∼2.5 nm). There are several reasonable explanations for this observation. First, the depth of the feature can be increased to ∼0.4−0.8 nm by scanning the pattern several times using standard imaging conditions (SIC) that do not affect unpatterned portions of the surface.[15] This suggests that some loosely bound hydrocarbon material remains in the pattern. Second, we believe that the STM tip penetrates the monolayer during normal imaging, so the apparent feature depth will be less than the thickness of the SAM.[14,31] Third, there may be differences in the density of electronic states of the Au in the patterned and unpatterned surface regions.[48] Importantly, the feature depth can be increased by repeating the patterning process: if patterning is continued long enough (typically >∼250 scans), the feature depth eventually becomes greater than the thickness of the SAM.[15] This indicates that, in addition to the SAM, the relatively chemically inert Au substrate can also be electrochemically etched.

Figure 1c is the image obtained after attempting to pattern a different region of the same SAM surface in dry air (6.6% RH) using the same conditions described for Figure 1b. With the exception of a slightly raised feature (+0.06 nm) in the patterned area, the surface remains unmodified. However, after reexposing the sample to humid air for 25 min, we were able to pattern the surface in a manner completely analogous to Figure 1b.

We obtained Figure 1d after patterning the surface in humid (78% RH) N_2. Patterning proceeds as it does in humid air. The depth (−0.25 nm) and RMS roughness factor (2.2) of the pattern formed in humid N_2 (Figure 1d) are very similar to those obtained in humid air (Figure 1b), which suggests that a similar patterning mechanism is operative in both media. The differences in the appearance, depth, and RRF between the patterns shown in Figure 1b,d are within the range of our limit of reproducibility and are thus indistinguishable. Figure 1e is an STM image obtained after patterning the ODM-coated Au(111) surface in dry N_2 (5% RH). As we observed in dry air,

SCHEME 1

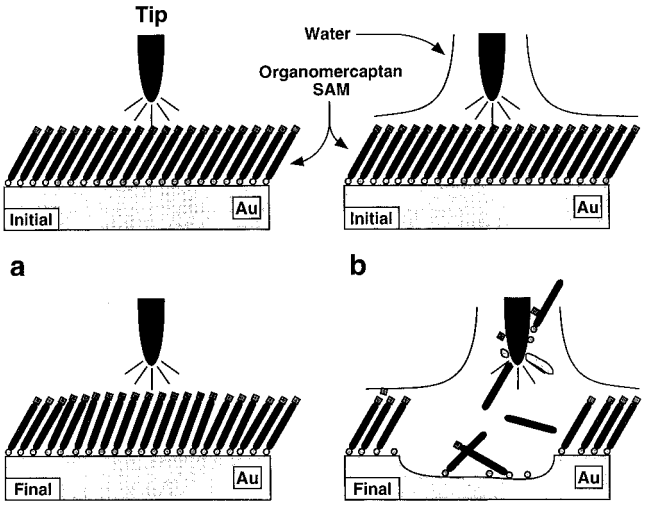

patterning does not occur at +3.0 V, except for the formation of a slightly raised area (+0.01 nm). Even when we increased the sample bias to +5.0 V (a bias at which extensive and irreproducible patterning and severe tip damage occur in a humid environment), patterning in dry N_2 generally results in no more than a slightly raised area surrounding somewhat enlarged indigenous pits. Our observation that patterning occurs only at elevated relative humidities, but is otherwise independent of the atmosphere, confirms that a common patterning mechanism is active in air and N_2, and therefore eliminates O_2, CO_2, and other species present in air as contributors to the patterning process.

We obtained the image in Figure 1f after patterning an ODM-coated Au(111) surface in humid air at −3.0 V. By reversing the polarity of the tip bias (substrate negative), we formed a raised feature that is much higher than those in Figure 1c,e. The small islands that comprise the feature suggest that material nucleates on the surface and then grows together to yield a single body. The height of the raised feature increases as a function of the patterning time, which is consistent with electrochemical deposition of material onto the surface. We can subsequently remove the deposited material by patterning it with a positive sample bias. However, it cannot be removed by repetitive scanning using SIC. Consistent with Figure 1a−e, deposition does not occur in low-humidity environments.

All of our observations are consistent with an electrochemical mechanism being responsible for the observed surface transformations. Scheme 1 illustrates the humidity-dependent mechanism that we believe leads to patterning. Part a of Scheme 1 shows that patterning does not occur in a dry (<∼25% RH) environment, because water does not condense to an appreciable extent on the surface or tip. As a result, there is insufficient electrolyte solution present to support Faradaic electrochemical processes. Part b of Scheme 1 shows that in a humid environment (>∼70% RH), a thin film of water is present on the low-energy, methylated surface of the SAM, or is dragged along by the hydrophilic tip, which establishes an ultra-thin-layer electrochemical cell in the vicinity of the tip. It is worth noting that at intermediate humidity levels the extent of patterning is intermediate between those shown in Figure 1b,c.[49]

Because of the hydrophobic nature of the SAM, we believe that the electrolyte solution layer is very thin and contains a very low concentration of current-carrying ions. As a result, migration and diffusion are severely hindered, except in the immediate vicinity of the tip, and there is a rapid increase in the resistance as the distance from the tip increases.[50] This advantageous condition distinguishes this method from scanning electrochemical microscopy[17−21] or the conventional approach to *in situ* electrochemical STM,[42,44,51−57] in which the entire tip and substrate are immersed in a high-ionic-strength solution. It also allows us to localize the electrochemistry to the immediate vicinity of the tip and introduces the possibility of a convenient way to study electrochemical phenomena on a 1−100 nm length scale.

At the present time, we are uncertain about the nature of the Faradaic electrochemistry that occurs at the tip and surface during patterning. Straightforward interpretation of current−voltage transients are hindered since the tip is in close proximity to the surface and the Faradaic current is therefore convoluted with tunneling current. The observed etching at positive sample biases is consistent with oxidative stripping of the SAM followed by anodic dissolution of the Au substrate after repeated patterning. Consistent with this model, it was recently reported that irreversible anodic stripping of organomercaptans from Au surfaces occurs at potentials greater than ∼0.8 V vs Ag/AgCl-(saturated KCl) in KOH solutions.[46,58] The processes shown in eqs 1 (pH < 4) and 2 (pH > 7) were proposed as possible

$$CH_3(CH_2)_nS{-}Au + 2H_2O \rightarrow Au(0) + CH_3(CH_2)_nSO_2H + 3e^- + 3H^+ \quad (1)$$

$$CH_3(CH_2)_nS{-}Au + 2H_2O \rightarrow Au(0) + CH_3(CH_2)_nSO_2^- + 3e^- + 4H^+ \quad (2)$$

stripping reactions. The products of these two reactions are much more loosely bound to the surface than mercaptans and therefore readily desorb: a similar process, probably aided by tip-induced disruption of the SAM, may occur during STM-induced patterning. This model makes two particularly attractive predictions. First, it provides a species (H^+), which is generated by SAM oxidation, that can be easily reduced at the cathode (STM tip). Second, H_2O is required for the reactions represented in eqs 1 and 2 to proceed, which is in accord with our results.

In addition to removing the SAM, it is also possible to use the STM to dissolve Au. As evidence of this, we have fabricated 3.2-nm-deep patterns that exceed the length of the ODM SAM.[15] This strongly implies a Faradaic process since the Au substrate, although relatively chemically inert, is removed under the same conditions that remove the SAM. We also considered, but for the present (at least) reject, an indirect etching mechanism whereby electrogenerated solution-phase species, such as peroxide or hydroxyl radicals generated by electrolysis of H_2O, react with the SAM. In such a scenario it seems unlikely that we would be able to etch both the SAM and the underlying Au substrate using identical sets of conditions.

Although we have not extensively studied the processes that lead to surface-deposited material at negative sample biases (Figure 1f), surface-bound organomercaptans are known to undergo reduction to form thiolates (eq 3).[46,47,58] In contrast

$$CH_3(CH_2)_nS{-}Au + e^- \rightarrow Au(0) + CH_3(CH_2)_nS^- \quad (3)$$

to oxidation, reduction is an electrochemically reversible process, and therefore we might not expect irreversible desorption of the thiol from the surface at negative sample biases in this constricted cell configuration. Also, since the deposited material results in a mound whose height can be controllably increased by prolonging or repeating the deposition process (for example, to 2.4 nm after 25 patterning scans), we know that it is at least

somewhat conductive. If it were not, we would be unable to tunnel into it. Since ODM is a bulk insulator, we believe that the deposited material must contain either Au from the surface or metal that has been electrochemically stripped from the tip and redeposited on the surface. However, it is likely that the primary component of the mound is ODM originally transferred to the tip from the SAM as a result of scanning and subsequently desorbed upon biasing the tip positive. Previously, it has been observed that Au can be deposited onto surfaces from Au STM tips by field evaporation.[59,60] While the fields generated in our experiments may be sufficiently high to change the tip shape,[61,62] it is unlikely that they are sufficient to cause field evaporation of Pt or Ir.

To better understand the role played by the organomercaptan SAM during the patterning process, we also examined patterning on *n*-nonyl mercaptan (NM)-coated Au(111) and nominally naked Au(111) surfaces. In humid environments both surfaces yield patterns that are much deeper, rougher, and more irregularly shaped compared to ODM-coated surfaces, but they do not etch in dry environments. Interestingly, patterns on the SAM-coated surfaces are stable, but those on naked Au begin to anneal immediately. This is consistent with the high mobility of Au surface atoms.[42−44,63−65] The extent of etching decreases in the order naked Au > NM-coated Au > ODM-coated Au. This is in agreement with previous electrochemical studies, which indicate that long-chain *n*-alkane mercaptan (e.g., ODM) monolayers passivate Au surfaces toward Faradaic processes more effectively than shorter, more poorly organized SAMs (e.g., NM).[23,24,30,66−77] The important points are that the SAMs improve pattern resolution and reproducibility, but they retard the rate of pattern development. Both of these results are fully consistent with our proposed model (Scheme 1).

To learn more about the processes responsible for feature formation, we performed pulse experiments, which eliminate effects on pattern formation that arise from lateral motion of the tip during scanning. Figure 2a is an STM image obtained after attempting to fabricate three features by applying 1 s duration, +3.0 V bias pulses with the tip held stationary.[16] We prepared the feature at location 1 in humid (75% RH) air. No feature was formed at location 2 in dry (6.0% RH) N_2. After reexposing the surface to humid air, we prepared the feature at location 3. The features at locations 1 and 3 are 8.6 and 9.4 nm in diameter, respectively, and 1.1 ± 0.1 nm deep, which demonstrates that this electrochemical method can be used to fabricate highly reproducible sub-10-nm-diameter patterns with volumes of less than 100 nm^3. The patterns are stable even after repeated STM scanning using SIC, and to the best of our knowledge, they are the smallest features intentionally fabricated in an organic thin film using an electrochemical technique.

Figure 2b is a plot of the likelihood of forming a feature as a function of the magnitude of the pulse bias (substrate positive). It shows that a distinct bias threshold must be exceeded to pattern either ODM-coated Au(111) or nominally naked Au(111) using a stationary tip. In humid air the threshold occurs at ∼+2.3 V for an ODM-coated surface, but at only ∼+2.0 V on a naked Au(111) surface. This dependence is consistent with direct electrochemical patterning of the surface and the passivating ability of organomercaptan SAMs.[23,24,30,66−77]

Figure 2c shows how the likelihood of patterning depends on the tip current. At biases below the threshold, no surface modification occurs regardless of the current or the total Coulomb dose. Since the patterning threshold does not depend on the tip current, we can rule out an exposure-based mechanism; that is, patterning does not result from bombardment of the surface by high-energy electrons as might be observed when using a focused electron beam in vacuum.

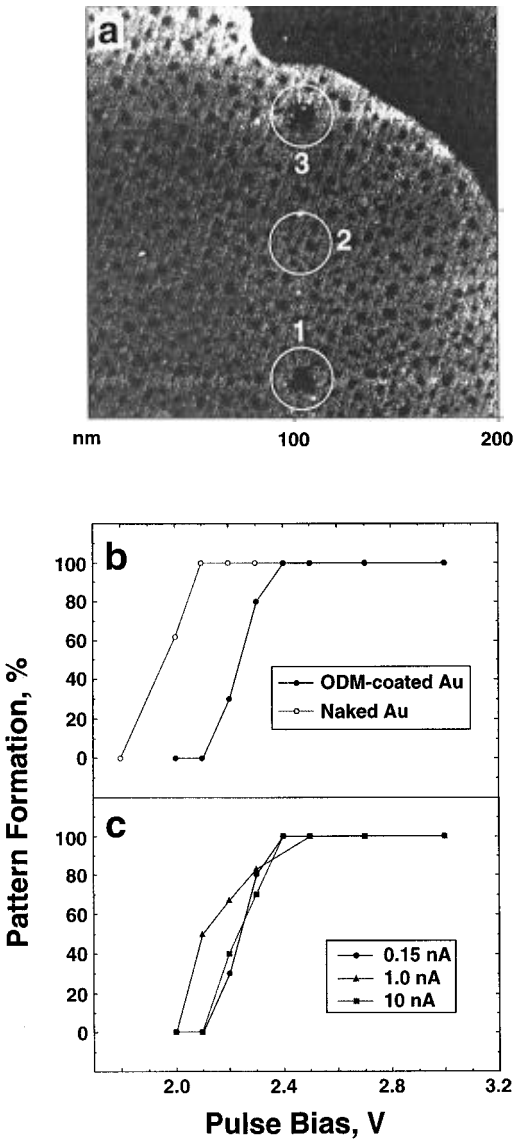

Figure 2. (a) 200 nm × 200 nm STM image of an *n*-octadecyl mercaptan SAM on Au(111) following the application of three 1 s, +3.0 V pulses with the tip held stationary. The gray scale is 2 nm. The circles are centered on the areas where the bias pulses were applied. The feature at location 1 was fabricated in humid (75% RH) air. No feature was formed at location 2 in dry (6.0% RH) N_2. The feature at location 3 was patterned after reexposing the surface to humid air. Patterns emerge only after application of bias pulses in the high-humidity ambient. (b) Plot of the likelihood of forming a surface feature as a function of the magnitude of the bias pulse applied to a stationary tip in humid air. A bias threshold of approximately +2.3 V is required for the ODM SAM (filled circles) while only about +2.0 V is required to pattern nominally naked Au(111) (open circles). The +0.3 V shift in the threshold clearly demonstrates the passivating ability of the *n*-octadecyl mercaptan SAM toward Faradaic electrochemical processes. Bias pulses in excess of ∼+3.5 V result in irreproducible patterning.[16] (c) Plot of the likelihood of forming a surface feature as a function of the magnitude of the bias pulse applied to a stationary tip in humid air at various tip currents. The duration of the current pulse was always 1 s. A bias threshold of approximately +2.3 V is required for the ODM SAM regardless of the current or total Coulomb dose.

Conclusion

In summary, we have presented evidence that STM-induced patterning of organomercaptan SAMs and nominally naked Au in air results from Faradaic electrochemical processes. We

believe the tip−substrate gap behaves as an ultra-thin-layer electrochemical cell in which the large IR drop through the SAM and surface-confined electrolyte restricts electrochemistry to a region defined by the instantaneous position of the tip. In this sense, the STM is acting as a high-resolution SECM.[17−21,78]

The monolayer plays three critical roles in controlling and improving the reproducibility and resolution of the patterns. First, the low-energy SAM minimizes the thickness of the water layer on the surface, which confines patterning to the immediate vicinity of the tip. As the length of the SAM backbone is reduced, the organization of the monolayer degrades, its surface energy increases, the thickness of the water layer increases, and the lateral pattern resolution decreases.[73,79] Second, the SAM passivates unetched regions of the Au surface, which promotes anisotropic etching. Third, the SAM retards the surface mobility of Au atoms and thereby stabilizes the pattern. The most important aspect of our results is that they suggest electrochemistry may be a very general and even dominant process when imaging conductive and insulating surfaces in air. Clearly, STM results obtained in humid environments must be evaluated with great care.

Finally, we believe the results presented here raise some very fundamental questions about electrochemical processes that occur in ultrasmall domains. For example, it is somewhat difficult to imagine using standard electrochemical models, such as Gouy−Chapman theory or any theory that presents the electrolyte solution as a continuum, to interpret results from cells with angstrom-scale dimensions: there are insufficient solvent and electrolyte molecules present for such macroscopic models to be relevant. There are also questions related to the structure of the solvent and quantities of electrolyte that might be present in the gap that must be addressed. It is also rather intriguing to speculate on whether solvent, H_2O in the case presented here, is necessary to support electrochemical reactions at such small electrode spacing if H_2O is not specifically implicated in the redox reaction (eqs 1 and 2). We are trying to address these issues at the present time.[15,16]

Acknowledgment. Full support of this research by the Office of Naval Research is gratefully acknowledged. J.K.S. gratefully acknowledges an IBM Manufacturing Research Fellowship. We thank Dr. Marion Alcorn from the TAMU meteorology department for use of the humidity/temperature sensor. We also thank Prof. Allen J. Bard (University of Texas) and Prof. Henry S. White (University of Utah) for thought-provoking suggestions and comments.

References and Notes

(1) Corbitt, T. S.; Crooks, R. M.; Ross, C. B.; Hampden-Smith, M. J.; Schoer, J. K. *Adv. Mater.* **1993**, *5*, 935−938.

(2) McCarley, R. L.; Hendricks, S. A.; Bard, A. J. *J. Phys. Chem.* **1992**, *96*, 10089−10092.

(3) Staufer, U. In *Scanning Tunneling Microscopy II*; Wiesendanger, R., Güntherodt, H.-J., Eds.; Springer-Verlag: New York, 1992; Vol. 28, pp 273−302 and references cited therein.

(4) Lebreton, C.; Wang, Z. Z. *Scanning Microsc.* **1994**, *8*, 441−448.

(5) Penner, R. M.; Heben, M. J.; Lewis, N. S.; Quate, C. F. *Appl. Phys. Lett.* **1991**, *58*, 1389−1391.

(6) Mizutani, W.; Inukai, J.; Ono, M. *Jpn. J. Appl. Phys.* **1990**, *29*, L815−L817.

(7) Albrecht, T. R.; Dovek, M. D.; Kirk, C. A.; Lang, C. A.; Quate, C. F.; Smith, D. P. E. *Appl. Phys. Lett.* **1989**, *55*, 1727−1729.

(8) Rabe, J. P.; Buchholz, S.; Ritcey, A. M. *J. Vac. Sci. Technol.* **1990**, *A8*, 679−683.

(9) Sugimura, H.; Uchida, T.; Kitamura, N.; Masuhara, H. *J. Phys. Chem.* **1994**, *98*, 4352−4357.

(10) Sugimura, H.; Uchida, T.; Kitamura, N.; Masuhara, H. *Appl. Phys. Lett.* **1993**, *63*, 1288−1290.

(11) Sugimura, H.; Uchida, T.; Kitamura, N.; Masuhara, H. *Jpn. J. Appl. Phys.* **1993**, *32*, L553−L555.

(12) Chan, K. C.; Kim, T.; Schoer, J. K.; Crooks, R. M. *J. Am. Chem. Soc.* **1995**, *117*, 5875−5876.

(13) Schoer, J. K.; Ross, C. B.; Crooks, R. M.; Corbitt, T. S.; Hampden-Smith, M. J. *Langmuir* **1994**, *10*, 615−618.

(14) Ross, C. B.; Sun, L.; Crooks, R. M. *Langmuir* **1993**, *9*, 632−636.

(15) Schoer, J. K.; Crooks, R. M. Submitted for publication in *Langmuir*.

(16) Schoer, J. K.; Crooks, R. M. Manuscript in preparation.

(17) Arca, M.; Bard, A. J.; Horrocks, B. R.; Richards, T. C.; Treichel, D. A. *Analyst* **1994**, *119*, 719−726.

(18) Bard, A. J.; Fan, F. R. F.; Mirkin, M. V. *Electroanal. Chem.* **1994**, *18*, 243−373.

(19) Bard, A. J.; Fan, F. R. F. *Faraday Discuss.* **1992**, *94*, 1−22.

(20) Bard, A. J.; Fan, F. R. F.; Kwak, J.; Lev, O. *Anal. Chem.* **1989**, *61*, 132−138.

(21) Bard, A. J.; Denuault, G.; Lee, C.; Mandler, D.; Wipf, D. O. *Acc. Chem. Res.* **1990**, *23*, 357−363.

(22) Snyder, S. R.; White, H. S. *J. Electroanal. Chem.* **1995**, *394*, 177−185.

(23) Chailapakul, O.; Crooks, R. M. *Langmuir* **1993**, *9*, 884−888.

(24) Crooks, R. M.; Chailapakul, O.; Ross, C. B.; Sun, L.; Schoer, J. K. In *Interfacial Design and Chemical Sensing*; Mallouk, T. E., Harrison, D. J., Eds.; American Chemical Society: Washington, DC, 1994; Vol. 561, pp 104−122.

(25) Sun, L.; Crooks, R. M. *J. Electrochem. Soc.* **1991**, *138*, L23−L25.

(26) Snyder, S. R. *J. Electrochem. Soc.* **1992**, *139*, 5C.

(27) Hsu, T.; Cowley, J. M. *Ultramicroscopy* **1983**, *11*, 239−250.

(28) The sample holder is similar to one designed by White et al. It is a brass block measuring 10 mm × 10 mm × 3 mm with a 4 mm diameter hole drill through the center of the block. Two set screws are aligned opposite each other and centered on the through hole. These screws can be used to anchor the sample in the middle of the through hole if desired. We cut a groove perpendicular to the set screws connecting the 4 mm through hole to the outside edge of the block. A third set screw is aligned perpendicular to the slot and serves to hold the sample in place.

(29) We define the RMS roughness factor (RRF) as RRF = (RMS roughness of the patterned area)/(RMS roughness of the unpatterned terrace).

(30) Images obtained in dry and humid environments were essentially identical. However, in dry environments the tip became fouled more quickly and efforts to "clean" the tip by applying a short bias pulse were much less effective.

(31) Chailapakul, O.; Sun, L.; Xu, C.; Crooks, R. M. *J. Am. Chem. Soc.* **1993**, *115*, 12459−12467.

(32) Poirier, G. E.; Tarlov, M. J. *Langmuir* **1994**, *10*, 2853−2856.

(33) Poirier, G. E.; Tarlov, M. J.; Rushmeier, H. E. *Langmuir* **1994**, *10*, 3383−3386.

(34) Poirier, G. E.; Tarlov, M. J. *J. Phys. Chem.* **1995**, *99*, 10960−10964.

(35) Sprik, M.; Delamarche, E.; Michel, B.; Röthlisberger, U.; Klein, M. L.; Wolf, H.; Ringsdorf, H. *Langmuir* **1994**, *10*, 4116−4130.

(36) Edinger, K.; Gölzhäuser, A.; Demota, G. K.; Wöll, C.; Grunze, M. *Langmuir* **1993**, *9*, 4−8.

(37) Anselmetti, D.; Gerber, C.; Michel, B.; Wolf, H.; Güntherodt, H.; Rohrer, H. *Europhys. Lett.* **1993**, *23*, 421−426.

(38) Schönenberger, C.; Sondag-Huethorst, J. A. M.; Jorritsma, J.; Fokkink, L. G. J. *Langmuir* **1994**, *10*, 611−614.

(39) The NanoScope software calculates the mean feature level in the roughness analysis feature by calculating the average of all the *z* values within a selected area relative to the *z* value of the tip when it is engaged.

(40) Wagner, F. T.; Ross, P. N. *J. Electroanal. Chem.* **1983**, *150*, 141.

(41) Wiechers, J.; Twomey, T.; Kolb, D. M. *J. Electroanal. Chem.* **1988**, *248*, 451−460.

(42) Trevor, D. J.; Chidsey, C. E. D.; Loiacono, D. N. *Phys. Rev. Lett.* **1989**, *62*, 929−932.

(43) Trevor, D. J.; Chidsey, C. E. D. *J. Vac. Sci. Technol.* **1991**, *B9*, 964−968.

(44) Honbo, H.; Sugawara, S.; Itaya, K. *Anal. Chem.* **1990**, *62*, 2424−2429.

(45) Honbo, H.; Itaya, K. *J. Chim. Phys.* **1991**, *88*, 1477−1489.

(46) Widrig, C. A.; Chung, C.; Porter, M. D. *J. Electroanal. Chem.* **1991**, *310*, 335−359.

(47) Weisshaar, D. E.; Lamp, B. D.; Porter, M. D. *J. Am. Chem. Soc.* **1992**, *114*, 5860−5862.

(48) Kim, Y.-T.; Bard, A. J. *Langmuir* **1992**, *8*, 1096−1102.

(49) Also, the first patterning cycle in a dry environment after the system has been exposed to a humid environment frequently forms a partial pattern. This is probably the result of residual water on the hydrophilic tip. Similarly, when returning to a humid environment, frequently only a partial pattern is formed if the system is not fully equilibrated with the ambient.

(50) Bard, A. J.; Faulkner, L. R. *Electrochemical Methods: Fundamentals and Applications*; John Wiley & Sons: New York, 1980; pp 8−10, 20−26.

(51) Suggs, D. W.; Bard, A. J. *J. Phys. Chem.* **1994**, *98*, 8349−8355.

(52) Suggs, D. W.; Bard, A. J. *J. Am. Chem. Soc.* **1994**, *116*, 10725−10733.
(53) Sashikata, K.; Furuya, N.; Itaya, K. *J. Vac. Sci. Technol.* **1991**, *B9*, 457−464.
(54) Hachiya, T.; Itaya, K. *Ultramicroscopy* **1992**, *42*−*44*, 445−452.
(55) Schardt, B. C.; Yau, S. L.; Rinaldi, F. *Science* **1989**, *243*, 1050−1053.
(56) Gao, X.; Weaver, M. J. *J. Am. Chem. Soc.* **1992**, *114*, 8544−8551.
(57) Li, W.; Duong, T.; Virtanen, J. A.; Penner, R. M. In *Nanoscale Probes of the Solid/Liquid Interface*; Gewirth, A. A., Siegenthaler, H., Eds.; Kluwer Academic Publishers: Boston, 1995; Vol. 288, pp 183−192.
(58) Walczak, M. M.; Popenoe, D. D.; Deinhammer, R. S.; Lamp, B. D.; Chung, C.; Porter, M. D. *Langmuir* **1991**, *7*, 2687−2693.
(59) McBride, S. E.; Wetsel, G. C. J. *Appl. Phys. Lett.* **1991**, *59*, 3056−3058.
(60) Mamin, H. J.; Guethner, P. H.; Rugar, D. *Phys. Rev. Lett.* **1990**, *65*, 2418−2421.
(61) Schott, J. H.; White, H. S. *Langmuir* **1993**, *9*, 3471−3477.
(62) Yokoi, N.; Ueda, S.; Namba, S.; Takai, M. *Jpn. J. Appl. Phys. 2* **1993**, *32*, L129−L131.
(63) Jaklevic, R. C.; Elie, L. *Phys. Rev. Lett.* **1988**, *60*, 120−123.
(64) Schneir, J.; Sonnenfeld, R.; Marti, O.; Hansma, P. K.; Demuth, J. E.; Hamers, R. J. *J. Appl. Phys.* **1988**, *63*, 717−721.
(65) Gjostein, N. A. In *Surfaces and Interfaces I*; Burke, J. J., Reed, N., Weiss, V., Eds.; Syracuse University Press: Syracuse, NY, 1966; pp 271−304.
(66) Finklea, H. O.; Snider, D. A.; Fedyk, J. *Langmuir* **1990**, *6*, 371−376.
(67) Finklea, H. O.; Avery, S.; Lynch, M.; Furtsch, T. *Langmuir* **1987**, *3*, 409−413.
(68) Finklea, H. O.; Snider, D. A.; Fedyk, J. *Langmuir* **1993**, *9*, 3660.
(69) Sabatani, E.; Rubinstein, I.; Maoz, R.; Sagiv, J. *J. Electroanal. Chem.* **1987**, *219*, 365−371.
(70) Sabatani, E.; Rubinstein, I. *J. Phys. Chem.* **1987**, *91*, 6663−6669.
(71) Miller, C. J.; Cuendet, P.; Gratzel, M. J. *J. Phys. Chem.* **1991**, *95*, 877−886.
(72) Strong, L.; Whitesides, G. M. *Langmuir* **1988**, *4*, 546−558.
(73) Bain, C. D.; Troughton, E. B.; Tao, Y.-T.; Evall, J.; Whitesides, G. M.; Nuzzo, R. G. *J. Am. Chem. Soc.* **1989**, *111*, 321−335 and references therein.
(74) Bain, C. D.; Whitesides, G. M. *J. Am. Chem. Soc.* **1989**, *111*, 7164−7175.
(75) Bain, C. D.; Evall, J.; Whitesides, G. M. *J. Am. Chem. Soc.* **1989**, *111*, 7155−7164.
(76) Li, Y.-Q.; Chailapakul, O.; Crooks, R. M. *J. Vac. Sci. Technol.* **1995**, *B13*, 1300−1306.
(77) Schoer, J. K. *Electrochem. Soc. Interface* **1995**, *4*, 56−57.
(78) Fan, F. R.; Bard, A. J. The University of Texas at Austin, personal communication.
(79) Whitesides, G. M.; Laibinis, P. E. *Langmuir* **1990**, *6*, 87−96.

JP960271P